Boundary-Layer Meteorol (2007) 124:61–79
DOI 10.1007/s10546-006-9146-5

ORIGINAL PAPER

Model evaluation of the atmospheric boundary layer and mixed-layer evolution

Maria Tombrou · Aggeliki Dandou · Costas Helmis · Evaggelos Akylas · George Angelopoulos · Helena Flocas · Vasiliki Assimakopoulos · Nikolaos Soulakellis

Received: 12 December 2005 / Accepted: 15 November 2006 / Published online: 24 January 2007

Abstract In the present study, an attempt is made to assess the atmospheric boundary-layer (ABL) depth over an urban area, as derived from different ABL schemes employed by the mesoscale model MM5. Furthermore, the relationship of the mixing height, as depicted by the measurements, to the calculated ABL depth or other features of the ABL structure, is also examined. In particular, the diurnal evolution of ABL depth is examined over the greater Athens area, employing four different ABL schemes plus a modified version, whereby urban features are considered. Measurements for two selected days, when convective conditions prevailed and a strong sea-breeze cell developed, were used for comparison. It was found that the calculated eddy viscosity profile seems to better indicate the mixing height in both cases, where either a deep convective boundary layer develops, or a more confined internal boundary layer is formed. For the urban scheme, the incorporation of both anthropogenic and storage heat release provides promising results for urban applications.

Keywords Atmospheric boundary layer · Eddy viscosity · Entrainment layer · Mixing height · MM5 model · Sea breeze

M. Tombrou (✉) · A. Dandou · C. Helmis · G. Angelopoulos · H. Flocas
Lab. of Meterology, Department of Applied Physics, National and Kapodistrian University of Athens, Build. Phys. V., University Campus, 157 84 Athens, Greece
e-mail: mtombrou@phys.uoa.gr

E. Akylas · V. Assimakopoulos
Institute for Environmental Research and Sustainable Development, National Observatory of Athens, Lofos Koufou, Penteli, 152 36 Athens, Greece

N. Soulakellis
Department of Geography, University of the Aegean, 811 00 Mytilene, Greece

1 Introduction

The practical and theoretical problems associated with the determination of the mixing height (MH), and sometimes even its definition, are reflected in the numerous definitions found in the literature (Stull (1988); Garratt 1992; Beyrich 1997; Seibert et al. 2000). A major problem is that the MH is not obtained by standard meteorological practices, and strongly depends on the available instrumentation. Moreover, it is often a non-specific parameter whose definition and estimation is not straightforward. For practical applications in environmental meteorology, the term MH is usually considered as equivalent to a depth scale of the boundary layer that is based on dynamical thermal or turbulent height scales, depending on the status of atmospheric stability (Beyrich 1997). Also, it is worth mentioning that a commonly used definition is that the MH defines the height above the surface up to which emitted air pollutants are diluted.

Inconsistencies in the MH estimation emerge from the use of meteorological dynamic models, which are considered as the most appropriate tool for determining MH, especially for strong horizontal inhomogeneity. In fact, up to now, existing meteorological models have been developed independently, without aiming at providing key information on MH for the dispersion models. Therefore, they usually provide the atmospheric boundary-layer (ABL) depth that defines the layer in which the effects of the surface are felt directly on time scales less than a day and in which significant fluxes are carried by turbulent motions (Garratt 1992). Given the above definitions of MH and ABL depth, it is clear that these two do not coincide in a number of atmospheric conditions. Besides, the ABL depth calculations depend strongly on the selected ABL parameterization scheme. On the other hand, recent ABL parameterization schemes, embodied in meteorological models, are based on quantities, such as the convective velocity scale, that are calculated from the MH and the surface sensible heat flux. It is not clear if the above mentioned parameters are used differently in meteorological models (e.g. Zhang et al. 2001).

In order to proceed further from the above general definitions and realize their practical incorporation in meteorological models, the structure of the ABL according to stability should be considered separately. The distinction between the stable boundary layer (SBL) and the convective boundary layer (CBL) is necessary because most of the methods used to compute the MH apply only to a specific stability regime. The intermediate asymptotic case with the heat flux approaching zero is often termed the neutral ABL.

According to Stull (1988), three layers can be identified within the CBL; the surface layer, the mixed layer and the entrainment zone. The whole CBL is often called the mixed layer (or the well-mixed layer), and its top is defined at the level of most negative heat flux, near the middle of the entrainment zone, or at the level where the capping inversion is strongest. Nevertheless, since turbulence extends beyond that height, one should be aware that the entrainment layer is not a well-mixed layer and the turbulent intensity declines toward its top (Gryning and Batchvarova 1994). Therefore, during convective conditions, there is a margin of tolerance regarding the MH and its determination. In particular, the MH can be related to, (i) the top of the entrainment zone (which can be reached by the emitted air pollutants), or to (ii) the middle of the entrainment zone (which represents a layer of substantial turbulence), or to (iii) the base of the entrainment zone (which corresponds to the well-mixed layer).

The SBL can be divided into two layers: a layer of continuous turbulence and an outer layer of sporadic or intermittent turbulence. Therefore, the MH during stable conditions corresponds to the top of the continuously turbulent layer, produced mainly by the wind shear. However, this does not always mean that turbulence is strictly confined to the region below the MH. One should be aware that for the SBL, aerosol layers associated with stratified turbulence can also be detected above the MH (Parameswaran 2001).

In the present study, the impact of different ABL approaches on the calculation of ABL depth is assessed. Furthermore, we attempt to relate the ABL depth to the MH, as depicted by the measurements or other features of the ABL structure. As a first step, the calculated ABL depth, based on turbulence parameters, could be considered as a candidate for the calculation of MH.

The spatial distribution of the ABL depth over the Greater Athens Area (GAA) is calculated using the mesoscale model MM5, considering several ABL parameterization schemes already incorporated in the model. In addition, the modified version of the MRF (medium-range forecast) ABL scheme (MRF-urban) (Dandou et al. 2005) is also applied, whereby urban features are considered. The results are compared to measurements derived from different approaches for two selected days. Convective conditions prevailed during both days, while a strong sea-breeze cell developed during the second examined day.

2 Methodology

2.1 Numerical simulations

Numerical simulations were performed with the non-hydrostatic, mesoscale model developed by PSU/NCAR, known as MM5, version V3-6-1, (Grell et al. 1994). The model includes a soil module, seven optional ABL schemes and eight optional microphysics schemes, with different degrees of complexity.

The MM5 numerical simulations were performed by applying two-way nesting. The first domain covers the extended area of Greece and the second domain is centred on the Attiki peninsula (Fig. 1). The 25-category USGS land-use classification scheme was adopted to provide land-cover data for the model domains. The initial and lateral boundary conditions for the outermost domain were provided by the European Center for Medium range Weather Forecast (ECMWF) numerical prediction model. While five choices for ABL schemes were explored (MRF, MRF-urban, Gayno-Seaman, Blackadar and Pleim-Xiu), the remaining model physics options were fixed. These included the use of the Grell cumulus scheme (Grell 1993) in the outermost domain (no cumulus parameterization in the inner domain), the simple ice explicit moisture scheme (Dudhia 1989), a cloud radiation scheme (Dudhia 1989), five-layer soil model (Dudhia 1996) (except from the Gayno-Seaman scheme and the Pleim-Xiu scheme that use their own land-surface and moisture sub-models).

The above applications were supplemented by information derived from satellite image analysis. In particular, two Landsat-5/TM images acquired on 13 June 1994 and 13 May 2003 covering the GAA, have been digitally processed and analysed in order to extract all urban elements that are greater than the size of the higher spatial resolution pixel (30 m). In this procedure, an updated and more realistic representation of the urban expansion was obtained. This detailed information was also used in the

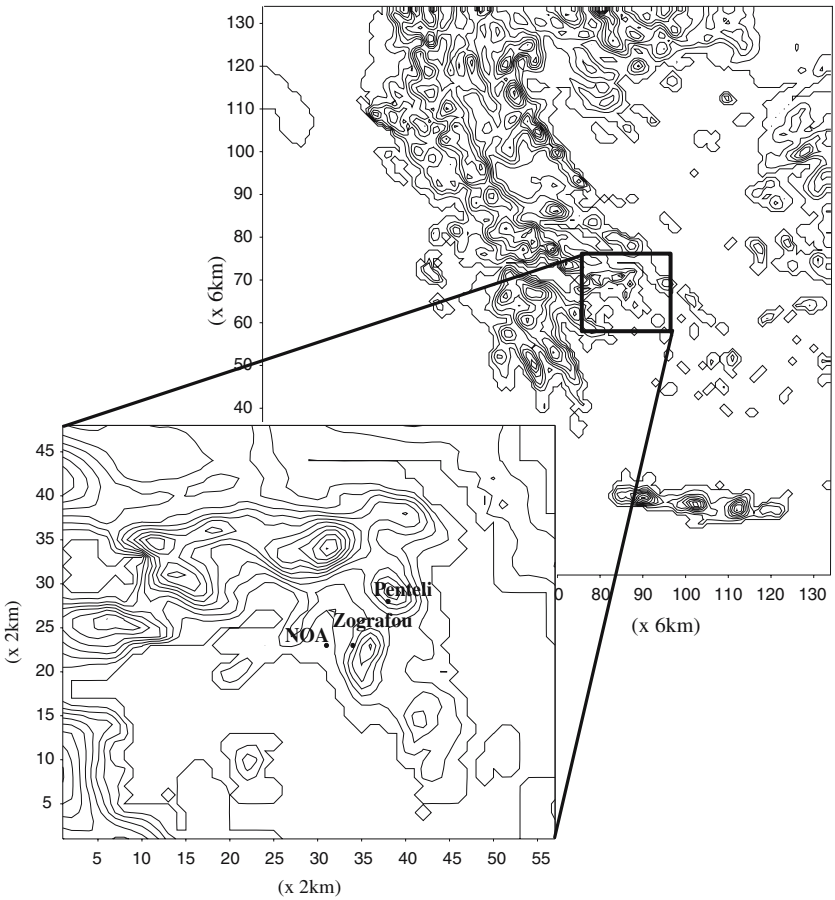

Fig. 1 Nested domain for modelling the Attiki peninsula and the position of three ground stations: NOA, Marousi and Penteli. The spatial resolutions are 6 and 2 km and the topography contour lines are every 100-m intervals for the Attiki peninsula and every 200-m intervals for the extended area of Greece

MRF-urban scheme in order to construct new fields for various parameters, such as the roughness length and the semi-empirical coefficients for the heat storage flux within the urban limits of the city, by applying an aggregation procedure. This was achieved by providing to each 30-m pixel (from the higher resolution domain) literature values (Grimmond et al. 1991; Grimmond and Oke 1999) for the various parameters, according to the above urban categories. Thereafter, these values were aggregated to each 4 km^2 grid cell in the MM5 modelling domain using an area-weighting scheme. Thus, the new values of the parameters in the modified version, reflect the presence of all the areas with different specifications within each 4 km^2 grid cell and are not related to a fixed land-use type.

2.2 ABL schemes in the MM5 model

For the present study, we have considered four different ABL parameterization schemes out of the seven total closure schemes: (a) the high resolution non-local MRF

scheme (Hong and Pan 1996), (b) the high resolution Blackadar's scheme (Zhang and Anthes 1982; Grell et al. 1994); (c) the Gayno-Seaman scheme (Musson-Genon 1987; Shafran et al. 2000), and (d) the more recent Pleim-Xiu scheme (Holtslag et al. 1990; Pleim and Chang 1992), a derivative of the Blackadar ABL scheme that uses a variation of non-local vertical mixing. In addition, the modified version of the MRF scheme (MRF-urban) (Dandou et al. 2005) is also applied, whereby urban features are considered. It should be mentioned that the urban areas are represented as bare soil with specific surface characteristics and physical parameters, such as roughness length, albedo etc in all these applications, apart from the MRF-urban scheme.

The characteristics of the ABL approaches have already been documented, and only a short description of the calculation of the ABL depth and eddy diffusivities is given below

The MRF ABL scheme (Hong and Pan 1996) is based on the Troen and Mahrt (1986) representation of the countergradient term in eddy diffusivities (K) and the K profile in the well-mixed ABL, as implemented in the medium-range forecast model (NCEP MRF). It is a first-order closure scheme, which is local in stable conditions. The turbulent fluxes in this scheme are calculated using the eddy diffusion method, but compared with the K-theory method, they contain an extra 'countergradient' term. This term is used to correct the turbulent heat flux in convective conditions, where large-eddy motions can produce a heat flux counter to the direction of the local temperature gradient (Holtslag and Moeng 1991). Under stable conditions, this term is small enough and can be neglected. In the mixed layer, the eddy viscosity is formulated as a function of friction velocity, the wind profile function evaluated at the top of the surface layer, the height and the ABL depth. The eddy diffusivity for temperature and moisture is computed from the eddy viscosity using the Prandtl number (Hong and Pan 1996). The top of the ABL is defined at the level of the minimum flux at the inversion level, described as an implicit function of the bulk Richardson number, the horizontal wind speed and the virtual potential temperature. This function also approximates the growth of the daytime mixed layer as well as allowing treatment of cases with weak surface heat flux and transitions between stable and unstable cases. This is achieved by relating the appropriate temperature near the surface to the temperature of thermals via the usual 'countergradient' flux correction for the unstable case (Troen and Mahrt 1986). In the case of vanishing wind speed and thus vanishing shear generation of turbulence, the function of the ABL depth becomes analogous to the thermodynamic approaches applied in Holzworth (1964) and Zhang and Anthes (1982). In the free atmosphere, the local diffusion Louis scheme (1979) is used. The schematic plot for the determination of the ABL depth, based on the virtual potential temperature profile, is presented in Fig. 2. In this figure, the ABL depth is determined both for unstable and stable conditions, according to Troen and Mahrt (1986).

MRF-urban ABL scheme (Dandou et al. 2005) is a modified version of the MRF ABL scheme whereby urban features have been introduced both in the thermal and dynamical parts. In particular, the released anthropogenic heat is given as a temporal and spatial function of the diurnal variation of the anthropogenic emissions, and the objective hysterisis model (OHM) (Grimmond et al. 1991) has also been incorporated for the calculation of the heat storage term. The surface fluxes were also modified according to Akylas et al. (2003) and Akylas and Tombrou (2005), following recent advances in knowledge of ABL structure over rough surfaces under unstable conditions. Finally, the eddy diffusivities for the stable cases were modified according to King et al. (2001).

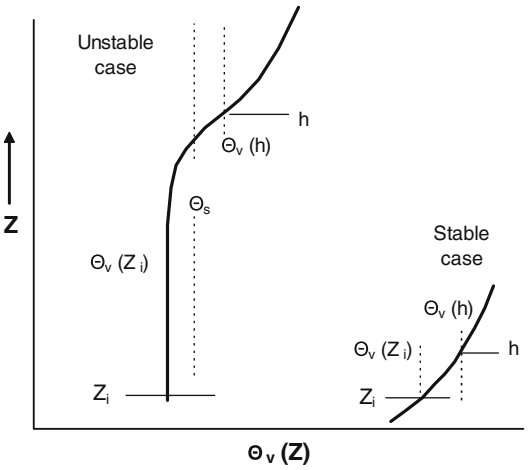

Fig. 2 Schematic diagram illustrating the ABL depth (h) relationship to the profile of the virtual potential temperature (Θ_v) above the surface (solid profile) for the MRF, MRF-urban and Pleim-Xiu schemes. For the unstable case, the first vertical broken line to the right of the profile indicates the virtual potential temperature after enhancement due to the temperature excess associated with surface heating (Θ_s). The second vertical broken line indicates the virtual potential temperature at the ABL top after deepening due to the shear-generated mixing as formulated in terms of a modified bulk Richardson number. The latter mechanism completely determines the depth of the stable ABL (after Troen and Mahrt 1986)

The Blackadar ABL scheme (Zhang and Anthes 1982; Grell et al. 1994) is representative of a non-local first-order closure approach for ABL large-eddy turbulence simulations and employs separate parameterizations (local and non-local approaches) for the nocturnal and free convection modules. The eddy diffusivities are calculated as functions of the Richardson number and the Blackadar length scale. Under stable conditions, wind-shear-driven turbulence and forced convection conditions, the turbulent fluxes are related to a local Richardson number, as derived by Blackadar (1976) from second-order closure theory. Under conditions of free convection, a non-local approach is employed to compute the ABL turbulent fluxes. Buoyant plumes of hot air rise from the surface layer and mix with air at each level within the ABL. Due to inertia, some plumes overshoot into the overlying inversion. In this regime, the turbulent fluxes are not determined by local gradients but by the thermal structure of the whole mixed layer. Since this non-local mixing approach does not use any additional prognostic equations for second-order moments, it is regarded as a first-order closure method. The top of the ABL is determined at the base of the temperature inversion in cases of forced convection ($Ri_B < 0$ and $z/L > -1.5$, where Ri_B is the bulk Richardson number and L the Obukhov length), while in cases of free convection ($Ri_B < 0$ and $z/L \leq -1.5$) it is determined at the level where the entrainment rate (the ratio of the negative area to the positive area on the thermodynamical diagram) is equal to 0.2. This is based on theoretical and observational studies, which indicate that, over homogeneous terrain, the downward heat flux due to entrainment is typically ≈20% of the surface flux (Tennekes 1975; Mahrt and Lenschow 1976; Stull 1976). During nighttime (stable conditions) and in cases with mechanical turbulence the ABL depth is set equal to zero. The turbulent fluxes above the ABL are computed using the K-theory approach with an implicit diffusion scheme in both modules.

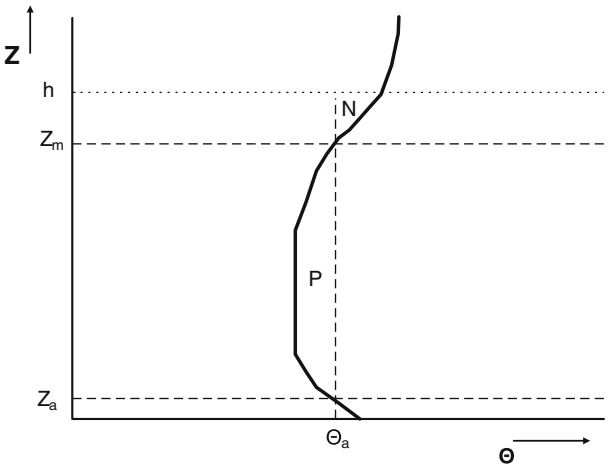

Fig. 3 Schematic diagram illustrating the ABL depth (h) relationship to the profile of potential temperature (Θ) above the surface (solid profile) for the Blackadar scheme, under free convection, where Z_a refers to the top of the surface layer (10 m) and Z_m to the level of zero buoyancy. The ratio of the negative area N to the positive area P is the entrainment rate. (after Zhang and Anthes 1982)

In Fig. 3, a schematic plot for the determination of the ABL depth (unstable conditions) is shown.

The Gayno-Seaman ABL scheme (Musson-Genon 1987; Shafran et al. 2000) is a Mellor-Yamada TKE-predictive 1.5-order closure scheme. As in the MRF scheme, the turbulent fluxes are calculated using the eddy diffusivity method but, compared with the K-theory method, they also contain an extra 'countergradient' term under convective conditions. The eddy diffusivities are functions of the turbulent kinetic energy (TKE) and the mixing length scales, as defined by Ballard et al. (1991). The scheme uses the liquid–water potential temperature as a conserved variable and not the generally used potential temperature, allowing the ABL to operate more accurately in saturated conditions (Ballard et al. 1991). The ABL depth is diagnosed from the TKE profiles with different treatments according to the value of maximum TKE within the ABL (Shafran et al. 2000). In general, the top of the ABL is the level where the TKE falls below a certain minimum threshold of 0.1 $m^2\,s^{-2}$ if the maximum TKE is larger than 0.2 $m^2\,s^{-2}$ (strong convection), otherwise, it is set to the level where the TKE decreases by 50% of its maximum value, when this is smaller than 0.2 $m^2\,s^{-2}$ (weak convection). In cases when the TKE is very weak (less than 0.04 $m^2\,s^{-2}$), the top of the ABL is set to the level of the lowest full sigma layer of the model, while under nighttime (stable) conditions the ABL depth is set equal to zero. The ABL depth is not presented as a schematic plot, since its calculation is based only on TKE thresholds.

The Pleim-Xiu ABL scheme (Pleim and Chang 1992) is a derivative of the Blackadar ABL scheme, also non-local in the CBL. It uses the asymmetric convective model non–local scheme, which is based on the concept that vertical transport within the CBL is inherently asymmetrical. Upward transport by buoyant plumes originating in the surface layer is simulated by mixing from the lowest model layer directly to all other layers in the CBL. Downward transport, however, proceeds only to the next lower layer in order to emulate gradual compensatory subsidence (Pleim and Chang 1992). The eddy diffusivity coefficients are based on Blackadar (1976), which is essentially the same as described in the Blackadar scheme. The ABL depth is determined according to Troen and Mahrt (1986), as in the MRF ABL scheme (Fig. 2). The difference lies in the determination of the constant of the 'countergradient' term in the eddy diffusivities and the critical bulk Richardson number is set to 0.25 instead of

0.5, due to the higher vertical resolution (Holtslag et al. 1990). Moreover, the virtual potential temperature in the function of the ABL depth is calculated at 2 m instead of the lowest half sigma model level ($\approx$36 m), as in the MRF scheme. This leads either to higher (under unstable conditions) or lower (under stable conditions) values of the ABL depth compared to the MRF scheme. In those cases, where the ABL depth falls to very low values in stable conditions, a minimum value is obtained according to Koracin and Berknowicz (1988).

Finally, given that the Blackadar and Pleim-Xiu schemes do not provide the eddy diffusivities for the unstable cases, the O'Brien (1970) method was applied directly to every set of simulation results. Through this approach, the eddy diffusivity coefficients are first determined at the top of the surface layer (10–100 m, the constant-flux layer), based on Louis (1979) relationships as a function of the mixing length, the vertical wind shear and a function of the Richardson number. Afterwards, their vertical structure through the ABL is calculated by using the O'Brien (1970) Hermite-interpolation profile method.

3 Numerical domain, meteorological conditions and measuring sites

The MM5 numerical simulations were performed by applying double nesting, with the first domain covering the extended area of Greece (804 km$\times$ 804 km) with spatial resolution 6 km$\times$6 km (134 $\times$ 134 grid points). The second domain covers the Attiki peninsula (114 km$\times$96 km), which encompasses the Saronic Gulf and Aigina Island to the south, Mt. Parnitha to the north, Pendeli and Hymettus mountains to the east (Fig. 1). The horizontal resolution applied to the second domain is 2 km$\times$2 km (57$\times$48 grid points). There are 22 non-uniform vertical layers, with the lowest level at around 30 m and the top layer at about 13 km.

For this study, the simulations were performed for 2 days:

(a) *20 September 2002*, which was selected from the EU-project ICAROS-NET experimental campaign. During that day, a large-scale surface anticyclone prevailed over the GAA, which resulted in fair weather conditions, weak synoptic flow from the north-western sector and low cloudiness of the cumulus type. According to a previous study by Helmis et al. (1995), under a westerly background flow that is perpendicular to the sea-breeze direction, the sea-breeze front is not well defined, and is accompanied by relatively weak, and delayed sea-breeze development. These characteristics have also been observed in this case, as the southerly/south-westerly sea-breeze circulation arrived at the National Observatory of Athens (NOA) (a downtown station located on top of a hill (107 m asl), 4 km inland from the shore) at around 1300 LST at a speed of 3–4 m s^{-1}. These characteristics and the slow inland penetration of the sea breeze allowed the development of a deep mixing layer.

Sodar measurements were performed during this day at two locations in the GAA. More specifically, a Sodar (type PA1)—RASS profilometer and a sodar system (PA2), both manufactured by REMTECH Inc, were in operation at Zografou, a suburban background site (inside the University campus, on the fringe of the city centre) and at the Penteli Mountain (450 m height) in the north-east of Athens respectively. The measured MH values at the Zografou site were obtained by the visual inspection (manual method) of the hourly profiles of the horizontal

wind speed and direction and the sodar acoustic received echo, combined with the estimated potential temperature profiles from the profilometer. More details on these methods can be found in Asimakopoulos et al. (2004). At the Penteli site the estimated MH values were automatically determined by the system, based on the calculation of the power spectrum of the vertical wind velocity at each level. The characteristic frequency (time scale) that corresponds to the most energetic eddies multiplied by the mean wind speed leads to a length scale that is rather close to the MH (REMTECH 1994; Keder 1999). The latter method is based on the interrelationship of the most energetic turbulent eddies with the MH, as suggested for the unstable boundary layer by Kaimal et al. (1982). It should be mentioned that, according to the evaluation of the different methods based on comparison with direct measurements, the reliability of the manual methods is quite good during both the daytime and nighttime, while the automated method showed good agreement with the direct measurements only during the daytime (Asimakopoulos et al. 2004). Due to this reason, the manual methods, (using the horizontal wind speed and direction and the acoustic received echo hourly profiles) were also performed and combined with the automated method at Pendeli site.

(b) *15 September 1994*, which was selected by the MEDiterranean CAmpaign of PHOtochemical Evolution (MEDCAPHOT-TRACE) experimental campaign (Ziomas 1998). For this day, apart from the surface measurements, tethered balloon soundings (a relatively robust technique for estimating the convective mixed-layer depth) were also available, up to a height of 600 m at the NOA station (Batchavrova and Gryning 1998). Estimations of MH, based on the energy considerations for the entrainment zone, are also presented in their study. It should be mentioned that the relatively low value of the MH during this day allowed the use of the tethersonde, which can measure meteorological parameters at heights below 900 m. On that day, the surface synoptic circulation over GAA was characterized by the ridge from an extended anticyclone centered over northern Africa, and the synoptic wind was weak from the northern sector. Due to the weak opposing background flow, the developed sea-breeze circulation was characterized by an intense front, penetrating inland with strong winds and covering the whole Athens basin. The sea breeze with a south/south-westerly direction reached NOA at 1000 LST and a maximum wind speed of 4–5 m s^{-1} was measured between 1200 LST and 1800 LST (Batchvarova and Gryning 1998). Therefore, these conditions favoured the development of a more confined internal boundary layer (IBL).

4 Mixing height and ABL depth

4.1 20 September 2002

Figure 4 shows the diurnal variation of the ABL depths produced by the five ABL schemes of MM5, at the suburban background station of Zografou. Also, measurements of MH, performed by the sodar-RASS system, are presented for comparison.

During the daytime, higher values of the ABL depth (around 1700 m) are found for the non-local ABL schemes of MRF, MRF-urban and Pleim-Xiu. The similarity between the results of MRF and Pleim-Xiu was expected for the daytime period,

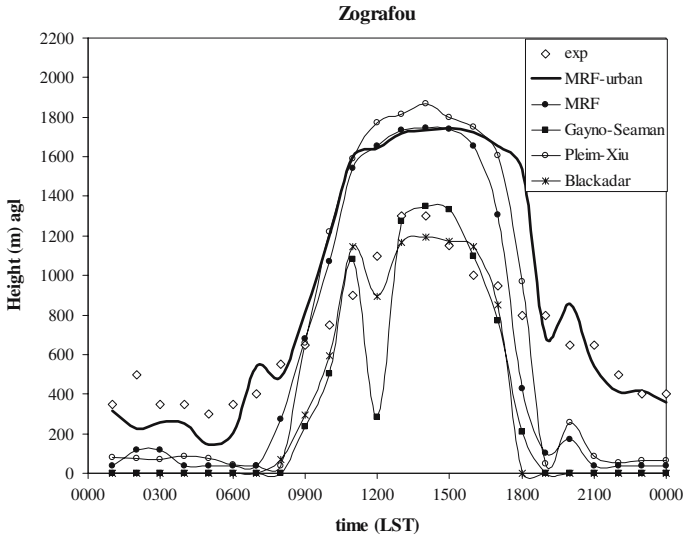

Fig. 4 The diurnal variation of MH as measured (diamonds) and calculated by the different ABL schemes of the MM5 model (solid lines) at Zografou site on 20 September, 2002

since both schemes involve the bulk Richardson number method according to Troen and Mahrt (1986). The results provided by the MRF-urban scheme did not alter the values of the ABL depth in comparison to the original version, with the only exception being the afternoon transition period where higher values are found. For the Gayno-Seaman and Blackadar schemes, the values of the ABL depth are much lower (less than 1400 m), with a slower growth rate than those for the MRF, MRF-urban and Pleim-Xiu schemes. However, their calculated values were very close to the measured values, especially during the period from 1000 LST to 1700 LST. Also, both schemes calculated an artificial decline of the ABL depth at 1200 LST, which is explained by the corresponding wind direction change from the north-western to south-western sector, resulting from the late sea-breeze development.

In order to determine the range of the thermal plume height according to the sodar signal, which is a measure of the altitude extent of the well-mixed region or otherwise the MH, the vertical structure of potential temperature and eddy viscosity are presented in Figs. 5 and 6, respectively. From the potential temperature profiles, as calculated by the various schemes at 1400 LST, it appears that the derived ABL depth values are mainly determined through the procedure that each ABL scheme applies for their calculation, and not through the substantial differences of the ABL structure, as already discussed in Sect. 2.2. The non-local approach of the Blackadar scheme is more efficient than that of Gayno-Seaman in generating a well-mixed thermal layer in the lower atmosphere, which is consistent with previous studies (Zhang et al. 2001; Fan and Sailor 2005). However, the temperature profile of the well-mixed layer (below 400 m), calculated by the Blackadar scheme, has lower values and therefore the values of the ABL depth derived from the Gayno-Seaman scheme are slightly higher, in contrast to the above mentioned studies. Finally, the Pleim-Xiu non-local approach is the most effective one in producing warmer and well-mixed thermal layer in the lower atmosphere, which explains the higher ABL depth values.

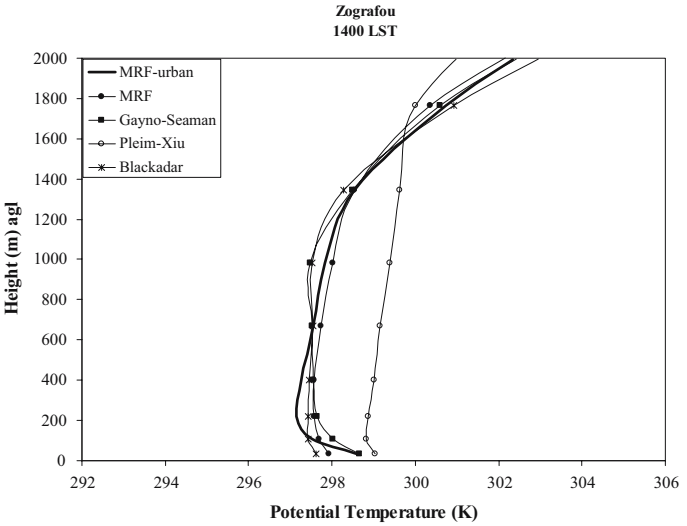

Fig. 5 Potential temperature profiles at 1400 LST as calculated by the different ABL schemes of the MM5 model at Zografou site on 20 September, 2002

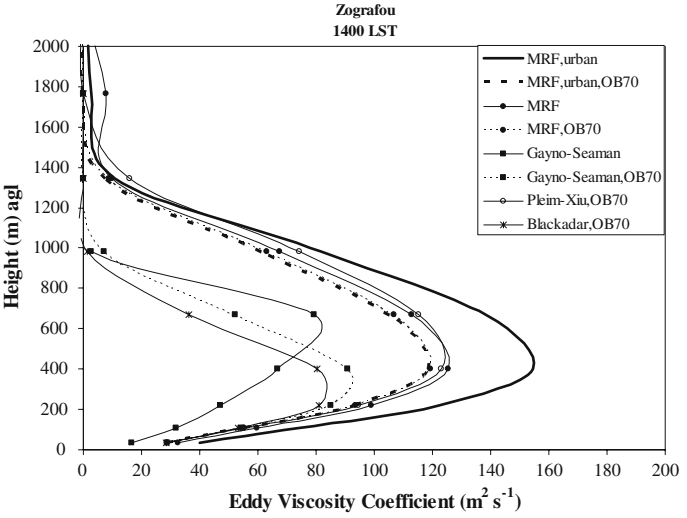

Fig. 6 Diffusion coefficient profiles at 1400 LST as calculated by the different ABL schemes of the MM5 model and by the O'Brien method (OB70) at Zografou site on 20 September 2002

A substantial acceleration of the diffusion processes is apparent in the MRF-urban results, as compared to the original version (Fig. 6). The modified profile functions, according to Akylas and Tombrou (2005), provide the major reason for this significant increase in the eddy viscosity at the suburban background site of Zografou. The combined effect of the anthropogenic heat and heat storage was not strong enough to compensate the dynamical changes, as occurred for the downtown station of NOA, during the other examined day (15 September 1994). The values of the ABL

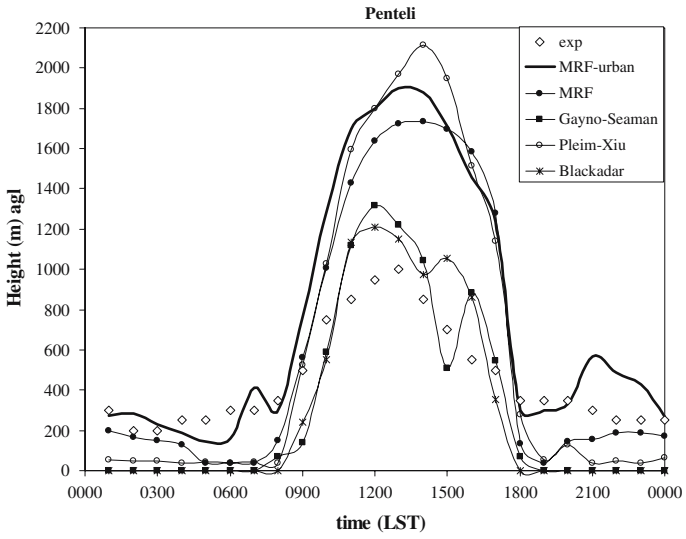

Fig. 7 As in Fig. 4 but for the Penteli site

depth, calculated by the less effective scheme of Gayno-Seaman, are higher than those calculated by the Blackadar scheme. This could also be explained by the fact that the maximum eddy viscosity value was calculated through the Gayno-Seaman scheme at higher levels (700 m). However, when the eddy viscosity profiles for these two schemes (Blackadar and Gayno-Seaman) were derived from the O'Brien (1970) method, they were found to be very similar and the larger values were provided from the Gayno-Seaman scheme.

Figure 7 shows the comparison among the diurnal variations of the ABL depth produced by the five ABL schemes of MM5 at the mountain station of Penteli. Measurements of MH, performed by the sodar (PA2) system, are also presented for comparison. During daytime, a similar behaviour appears between the various schemes, as presented at the Zografou site. Higher values of ABL depth (around 1800–2100 m) are found for the non-local ABL schemes of MRF, MRF-urban and Pleim-Xiu. Lower values (less than 1300 m), which were closer to the measurements, are found for the Gayno-Seaman and Blackadar schemes. The MRF-urban scheme altered the values of the ABL depth in comparison to the original version, producing much higher values especially between 0800 LST and 1500 LST. Nevertheless, according to the potential temperature profiles (Fig. 8), a weak temperature inversion is formed by the MRF-urban, around 900 m height, where the measured MH values were also recorded. The Gayno-Seaman scheme calculated also an artificial decline of the ABL depth at 1500 LST (Fig. 7), which is attributed to the change of the wind direction from the western to the northern sector (not shown) at the top of the ABL.

The vertical structure of the eddy viscosity for the Penteli site at 1400 LST is presented in Fig. 9. The substantial growth of the diffusion processes in the MRF-urban results, in comparison to the original version, can mainly be attributed to the modified profile functions, according to Akylas and Tombrou (2005), as discussed in Fig. 6. The Gayno-Seaman ABL scheme, on the other hand, calculates much lower values of eddy viscosity, compared to those calculated at the Zografou site. This scheme

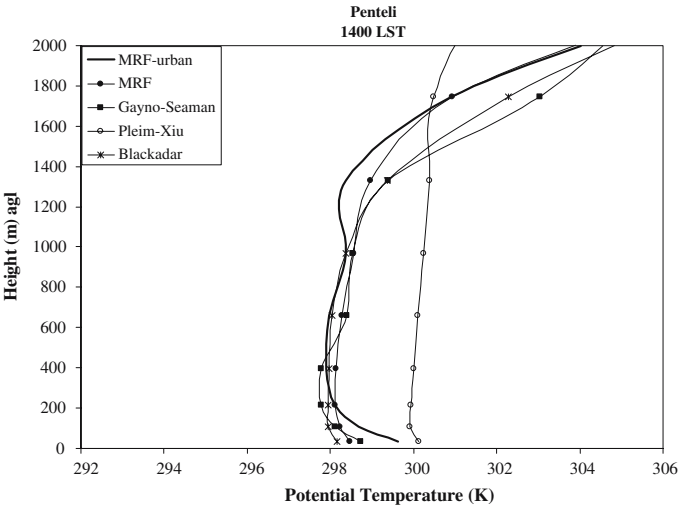

Fig. 8 As in Fig. 5 but for the Penteli site

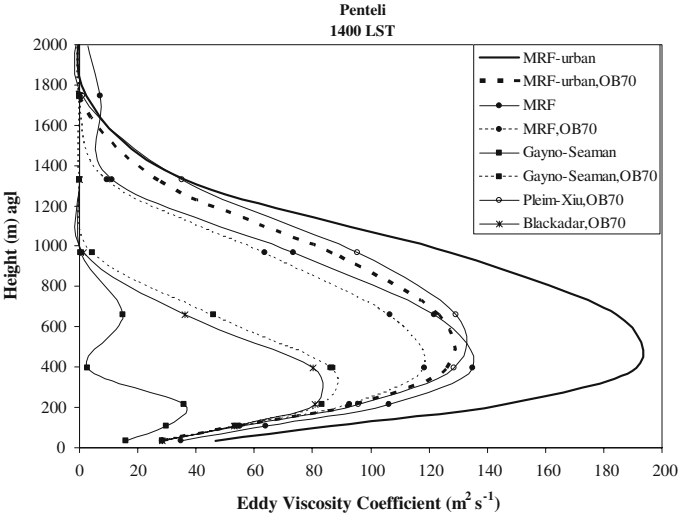

Fig. 9 As in Fig. 6 but for the Penteli site

produces less turbulence through the ABL than the other schemes and together with the Blackadar scheme they calculate lower values of the ABL depth. The small difference (higher values by the Gayno-Seaman scheme compared to the ones calculated by the Blackadar scheme) that appears at 1400 LST (Fig. 7) could be explained by the fact that when the eddy viscosity profiles were calculated by the same method (O'Brien 1970), the results almost coincided and the larger values were provided from the Gayno-Seaman scheme.

Reliable MH calculations could also be retrieved from the non-local ABL schemes (MRF, MRF-urban and Pleim-Xiu) if the eddy viscosities were employed. In this case, the middle of the entrainment zone (taken as the middle distance between

the maximum eddy viscosity value and the level where this diminishes) defines satisfactorily the top of a layer with substantial turbulence; therefore, it could be claimed that it corresponds to the MH values measured by sodar. Nevertheless, it should be noticed that if this approach is applied for the schemes of Gayno-Seaman and Blackadar (O'Brien method), the MH could be underestimated.

During the night, most of the calculated ABL depths approach zero or near-zero values. Only for the MRF-urban scheme are the results close to the sodar measurements at both locations, in contrast to the original MRF scheme. During the late evening hours, both measured and calculated values fluctuate around 500 m at Zografou while at Penteli they vary between 300 and 500 m (Figs. 4 and 7). The incorporation of both anthropogenic and storage heat releases into the lower atmosphere increases the air temperature in the urban canopy. This results in the development of an unstable layer near the surface, which is more evident at the Zografou station (not shown). At the same time, the eddy viscosity increased leading to more efficient mixing, especially within the first 200–300 m, at 0300 LST (not shown).

4.2 15 September 1994

During this day, the penetration of the sea-breeze advects cool air from the sea over the land, modifying the existing temperature structure and leading to the formation of a profound IBL, the height of which was calculated around 200 m at 0944 LST, using tethered balloon soundings of Batchavrova and Gryning (1998) at the NOA site. In this case, the onset of a strong IBL impedes significantly the penetration of eddies above its height and strong ABL mixing is confined to the region below. Fig. 10 shows the comparison between the diurnal variations of the ABL depth produced with the five ABL schemes, at the NOA station and the calculations of the IBL depth.

During the daytime, the calculated ABL depths are widely spread, in contrast to the previous day's results. Nevertheless, higher values (1700 m) are still estimated by the

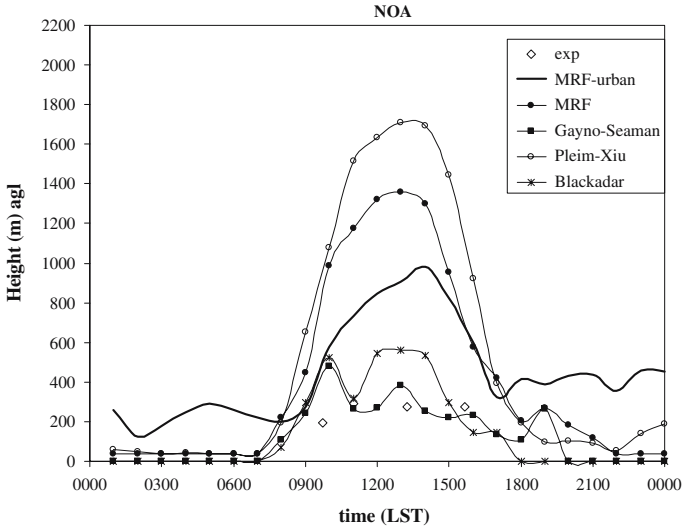

Fig. 10 As in Fig. 4 but for the NOA site on 15 September, 1994

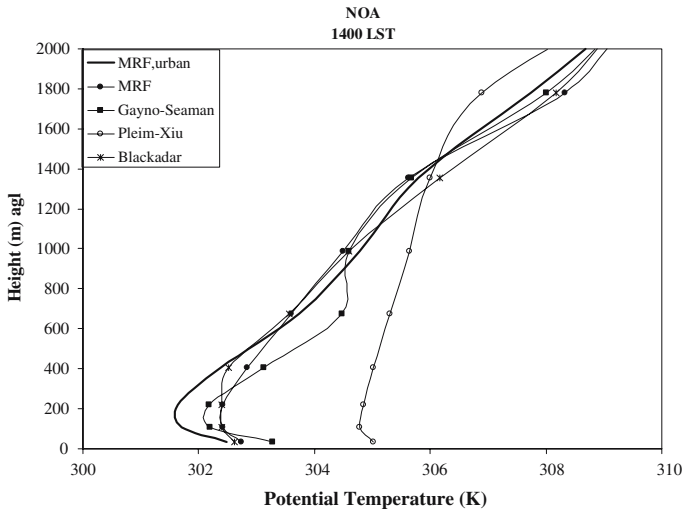

Fig. 11 As in Fig. 5 but for the NOA site on 15 September, 1994

Pleim-Xiu scheme, with lower ones by the Gayno-Seaman (300–400 m) and Blackadar (300–550 m) schemes. The corresponding values derived from Gayno-Seaman are in good agreement with the IBL depth, as this was estimated from measurements obtained by a tethersonde system, especially from 1100 to 1700 LST. Furthermore, this scheme depicts also changes or 'pulsations' of the IBL depth with time due to different land fetches that are caused by the irregular coastline and the changing wind direction, as observed and modelled by Batchavrova and Gryning (1998).

The results provided by the MRF-urban scheme show apparent changes both on the ABL depth and on the vertical structure of the lower atmosphere (Figs. 11 and 12). In particular, at the NOA site the potential temperature profiles, as calculated from the MRF-urban scheme, show that during the noon hours (1400 LST) the unstable layer is more intense than the original one, extending up to the height of 200 m and accompanied by an intense inversion (Fig. 11). This result coincides with the information derived from the measurements according to Batchavrova and Gryning (1998). The IBL depth reduction is also evident from the eddy viscosity profiles (Fig. 12), consistent with a reasonable decrease in their values.

The comparison between the estimated IBL depths and the eddy viscosity profiles (Fig. 12), demonstrates a perfect match with the levels where these coefficients obtain their maximum values, when the Blackadar and MRF-urban schemes are employed. This fact justifies the Parameswaran (2001) claim that the well-mixed region is closely associated with the height of the IBL. According to the same researcher, above this height, where the eddy viscosity decreases rather slowly with height, the entrainment region is formed. Inside the whole mixed layer, the onshore flow (from the south-west) is coupled with a balancing offshore flow aloft (from the north), as shown in Fig. 13.

The Gayno-Seaman ABL scheme was less turbulent near the surface, thus providing the lower values of ABL depth. If the O'Brien (1970) method is applied, larger values are calculated as compared to the original ones.

During the night, most of the calculated ABL depths approach zero or near-zero values, especially during the early morning hours. In the case of the MRF-urban

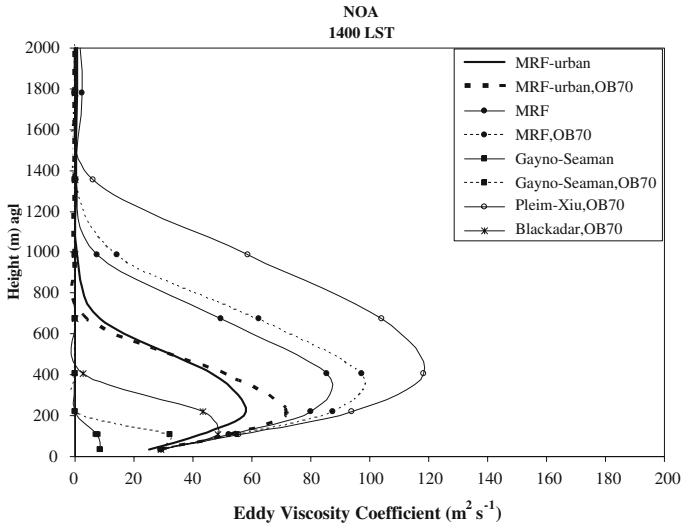

Fig. 12 As in Fig. 6 but for the NOA site on 15 September, 1994

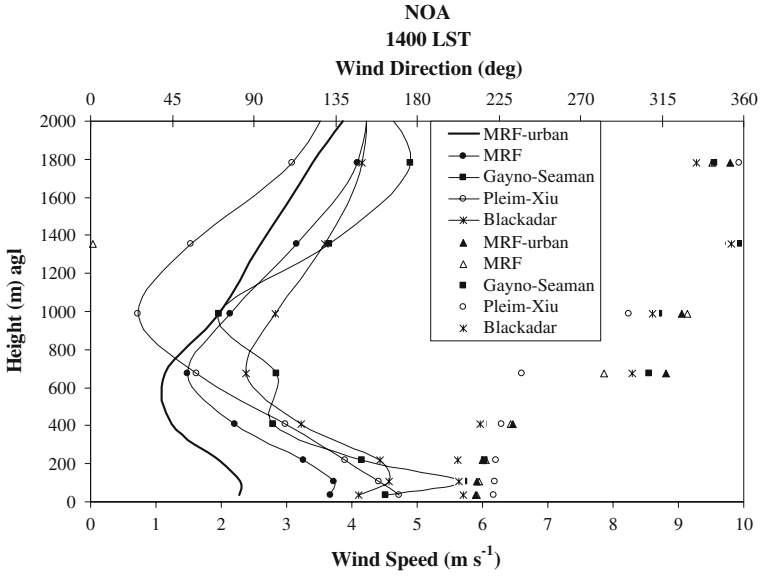

Fig. 13 Wind velocity (solid lines) and direction (separate symbols) profiles at 1400 LST as calculated by the different ABL schemes of the MM5 model at the NOA site on 15 September 1994

scheme the ABL depth reaches 500 m during the late evening hours. A much more pronounced unstable layer near the surface is formed by the same scheme, as shown from the potential temperature profile (Fig. 14). At the same time, the eddy viscosity is increased leading to a more efficient mixing capacity, especially within the first 150–200 m (not shown).

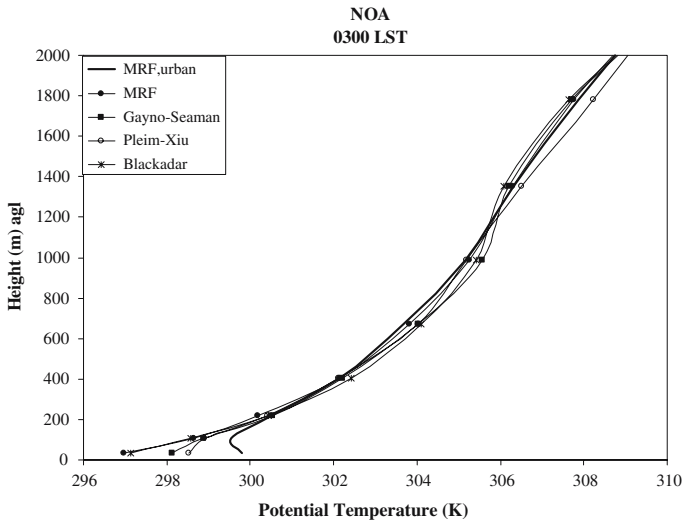

Fig. 14 As in Fig. 5 but for the NOA site at 0300 LST on 15 September, 1994

5 Conclusions

In this study the impact of different ABL parameterization schemes on the simulated ABL depth is assessed over an urban area and the calculated results were compared with measurements for two days. The differences in calculated ABL depths as derived from different ABL schemes are due to the fact that no unique definition is applied. It was found that the non-local schemes MRF, MRF-urban and Pleim-Xiu, which apply the same definition, generally provide higher values of the ABL depth during the daytime. This can be attributed to the fact that the non-local schemes effectively transport the buoyant plumes, originating in the surface layer directly to all other layers in the CBL. Best comparison with MH measurements is obtained when the ABL top is determined according to the Blackadar or the Gayno-Seaman scheme.

When the non-local schemes are applied under deep mixing conditions, the MH (as measured by the sodar) could be estimated in the middle of the entrainment layer, through the eddy viscosity profile. The ABL depth calculated by the local Gayno-Seaman scheme is closer to the experimental measurements of MH. When a more pronounced sea-breeze circulation is formed, the local scheme of Gayno-Seaman provides ABL depths corresponding to the IBL. However, a good correspondence was found between the IBL top and the level where the eddy viscosities obtain their maximum values, according to Blackadar and MRF-urban schemes, justifying the assumption that the well-mixed region is closely associated with the depth of the IBL. Therefore, it was demonstrated that the procedure that is based on the eddy viscosity profile seems to better represent the MH estimation in both cases.

During the night (stable conditions) there is an urgent need to involve better parameterization schemes, since the majority of the ABL schemes employ zero default values. For the MRF-urban scheme, the incorporation of both anthropogenic heat and heat storage, released into the lower atmosphere, increases the air temperature in the urban canopy, and consequently, the efficiency of the mixing mechanism. The MRF-

urban scheme seems to perform better in the city centre due to the incorporation of both anthropogenic and storage heat release into the lower atmosphere.

Acknowledgements We are grateful to the COST Action 715 'Meteorology applied to urban air pollution problems' activities which actually inspired this study. The experimental campaign was funded by the European Commission project ICAROS-NET (Integrated Computational Assessment via Remote Observation System NETwork) under grant IST-2000–29264.

References

Akylas E, Tsakos Y, Tombrou M, Lalas DP (2003) Considerations on minimum friction velocity. Quart J Roy Meteorol Soc 129:1929–1943

Akylas E, Tombrou M (2005) Reconsidering and generalized interpolation between Kansas-type formulae and free convection forms. Boundary-Layer Meteorol 115:381–398

Asimakopoulos DN, Helmis CG, Mihopoulos J (2004) Evaluation of sodar methods for the determination of the atmospheric boundary layer mixing height. Meteorol Atmos Phys 85:85–92

Ballard SP, Golding W, Smith R (1991) Mesoscale model experimental forecasts of the Haar of the Notheast Scotland. Mon Wea Rev 119:2107–2123

Batchvarova E, Gryning S.-E (1998) Wind climatology, atmospheric turbulence and internal boundary-layer development in Athens during the MEDCAPHOT-TRACE experiment. Atmos Environ 32(12):2055–2069

Blackadar AK (1976) Modeling the nocturnal boundary layer Preprints, 3rd Symp. On Atmospheric Turbulence, Diffusion and Air quality, Raleigh, Amer Meteorol Soc 38:283–290

Beyrich F (1997) Mixing height estimation from sodar data—a critical discussion. Atmos Environ 31(23):3941–3953

Dandou A, Tombrou M, Akylas E, Soulakellis N, Bossioli E (2005) Development and evaluation of an urban parameterization scheme in the Penn State/NCAR Mesoscale Model (MM5), J Geophys Res 110:D10102 (doi: 10.1029/2004JD005192)

Dudhia J (1989) Numerical study of convection observed during the winter monsoon experiment using a mesoscale two-dimensional model. J Atmos Sci 46:3077–3107

Dudhia J (1996) A multi-layer soil temperature model for MM5. Preprints, the 6th PSU/NCAR Mesoscale Model Users, Workshop, Boulder CO, July, National Center for Atmospheric Research, pp 49–50

Fan H, Sailor DJ (2005) Modeling the impacts of anthropogenic heating on the urban climate of Philadelphia: a comparison of implementations in two ABL schemes. Atmos Environ 39:73–84 (doi:10.1016/j.atmosenv.2004.09.031)

Garratt JR, (1992) The atmospheric boundary layer. Cambridge University Press, UK, 316 pp

Grell GA, (1993) Prognostic evaluation of assumptions used by cumulus parameterizations. Mon Wea Rev 121:764–787

Grell GA, Dudhia J, Stauffer D (1994) A description of the fifth-generation Penn state/NCAR mesoscale model (MM5). NCAR technical note, NCAR/TN-398 +STR, National Centre for Atmospheric Sciences, Boulder , CO, 138 pp

Grimmond CSB, Cleugh HA, Oke TR (1991) An objective urban heat storage model and its comparison with other schemes. Atmos Environ Part B 25:311–326

Grimmond CSB, Oke TR (1999) Heat storage in urban areas: Local scale observations and evaluation of a simple model. J Appl Meteorol 38:922–940

Gryning S-E, Batchvarova E (1994) Parametrization of the depth of the entrainment zone above the daytime mixed layer. Quart J Roy Meteorol Soc 120:47–58

Helmis CG, Papadopoulos KH, Kalogiros JA, Soilemes AT, Asimakopoulos DN (1995) Influence of background flow on evolution of Saronic Gulf sea breeze. Atmos Environ 29(24):3689–3701

Holtslag AAM, De Bruijn EIF, Pan HL (1990) A high resolution air mass transformation model for short-range weather forecasting. Mon Wea Rev 118:1561–1575

Holtslag AAM, Moeng CH (1991) Eddy diffusivity and counter-gradient transport in the convective atmospheric boundary layer. J Atmos Sci 48:1690–1698

Holzworth GC (1964) Estimates of mean maximum mixing depths in the contiguous United States. Mon Wea Rev 92:235–242

Hong SY, Pan HL (1996) Nonlocal boundary layer vertical diffusion in a medium-range forecast model. Mon Wea Rev 124:2322–2339

Kaimal JC, Abshire NL, Chadwick RB, Decker MT, Hooke WH, Kroepfli RA, Neff WD, Pasqualucci F, Hilderbrand PH (1982) Estimating the depth of the daytime convective boundary layer. J Appl Meteorol 21:1123–1129
Keder J (1999) Detection of inversions and mixing height by REMTECH PA2 sodar in comparison with collocated radiosonde measurements. Meteorol Atmos Phys 71:133–138
King JC, Connolley WM, Derbyshir SH (2001) Sensitivity of modeled Antarctic climate to surface and boundary-layer flux parameterizations. Quart J Roy Meteorol Soc 127:779–794
Koracin, D. Berkowicz R (1988) Nocturnal boundary-layer height: observations by acoustic sounders and predictions in terms of surface parameters. Boundary-Layer Meteorol 43:65–83
Louis JF (1979) A parametric model of vertical eddy fluxes in the atmosphere. Boundary-Layer Meteorol 17:187–202
Mahrt LJ, Lenschow DH (1976) Growth dynamics of the convectively mixed layer. J Atmos Sci 33:41–51
Musson-Genon L (1987) Numerical simulation of a fog event with a one dimensional boundary layer model. Mon Wea Rev 115:592–607
O'Brien JJ (1970) A note on the vertical structure of the Eddy Exchange Coefficient in the Planetary Boundary Layer. J Atmos Sci 27:1213–1215
Parameswaran K (2001) Influence of micrometeorological features on coastal boundary aerosol characteristics at the tropical station, Trivandrum. Proc Indian Acad Sci (Earth Planet Sci.) 110:247–265
Pleim JE, Chang JS (1992) A non-local closure model for vertical mixing in the convective boundary layer. Atmos Environ 26A:965–981
REMTECH (1994), DT /94/003 Remtech Doppler Sodar Operating Manual, Remtech Inc., Longmont, USA 27 pp
Shafran PC, Seaman NL, Gayno GA (2000) Evaluation of numerical predictions of boundary layer structure during the lake Michigan ozone study. J Appl Meteorol 39:412–426
Seibert P, Beyrich F, Gryning, S-E, Joffre S, Rasmussen A, Tercier Ph (2000) Review and intercomparison of operational methods for the determination of the mixing height. Atmos Environ 34:1001–1027
Stull RB (1976) Mixed-layer depth model based on turbulent energetics. J Atmos Sci 33:1268–1278
Stull RB (1988) An introduction to boundary layer meteorology. Atmospheric Sciences Library, Kluwer Academic Publ., Dordrecht, The Netherlands, 666 pp
Tennekes H (1975) Reply. J Atmos Sci 32:992–995
Troen I, Mahrt L (1986) A simple model for the atmospheric boundary layer: sensitivity to surface evaporation. Boundary-Layer Meteorol 37:129–148
Zhang D, Anthes RA (1982) A high-resolution model of the planetary boundary layer- sensitivity tests and comparisons with SESAME-79 data. J Appl Meteorol 21:1594–1609
Zhang K, Mao H, Civerolo K, Berman S, Ku Y.-Y, Rao ST, Doddridge B, Philbrick CR, Clark R (2001) Numerical investigation of boundary layer evolution and nocturnal low-level jets: local versus non-local ABL schemes. Environ Fluid Mech 1:171–208
Ziomas IC (1998) The Mediterranean campaign of photochemical tracers-transport and chemical evolution (MED-CAPHOT-TRACE): an outline. Atmos Environ 32:2045–2053